

## 2. EXPLANATORY NOTES<sup>1</sup>

C. Wylie Poag, U.S. Geological Survey, Woods Hole  
and  
Glen Foss, Scripps Institution of Oceanography<sup>2</sup>

### RESPONSIBILITY FOR AUTHORSHIP

The authorship of the site chapters is collectively the shipboard party, with ultimate responsibility lying with the co-chiefs, who rewrote parts of these chapters. All the site chapters follow essentially the same format. The authorship of individual sections is as follows:

Principal results—Graciansky, Poag  
Site approach and operations—Graciansky, Poag, Foss  
Sediment lithology—Graciansky, Loubere, Masson, Mazzullo, Ot-suka, Reynolds, Vaos  
Biostratigraphy:  
  Summary—Snyder  
  Cenozoic foraminifers—Snyder  
  Mesozoic foraminifers—Sigal  
  Nannoplankton—Müller  
Sediment accumulation rates—Müller, Poag  
Organic geochemistry—Cunningham, Waples  
Basalt lithology—Graciansky  
Paleomagnetism—Townsend  
Downhole logging—Graciansky  
Correlation of seismic profiles with drilling results—Montadert  
Summary and conclusions—Graciansky, Poag  
Appendix for Site 550 chapter—Montadert

Most of the observations, measurements, and conclusions given in the site chapters are based entirely on shipboard studies. Some sections were improved by incorporating shore-based studies, but readers should refer to the specialty chapters for the most complete, detailed, and up-to-date results.

### SURVEY AND DRILLING DATA

#### Site Surveys

Each drill site was chosen on the basis of survey data discussed in the site chapter. On passage between sites, continuous observations were made of depth, magnetic field, and sub-bottom structure. We used a precision echo sounder, seismic profiles, and a magnetometer to make short surveys with *Glomar Challenger* before dropping the beacon.

Depths were continuously recorded underway on a Giffit precision graphic recorder. The water depth (in m) at each site was corrected (1) according to the tables of Matthews (1939) and (2) for the depth of the hull transducer below sea level (6 m). Depths referred to the drill-

ing platform have been calculated on the assumption that the platform is 10 m above the waterline.

The seismic profiling system consisted of two Bolt air guns, a Scripps-designed hydrophone array, Bolt amplifiers, two bandpass filters, and two Edo recorders. The recorders were usually kept at different filter settings.

#### Drilling Characteristics

Because water circulation down the hole is open, cuttings are lost onto the seabed and cannot be examined. Thus, the only source of information about sedimentary stratification between cores, other than seismic data and downhole geophysical logs, is the behavior of the drill string as observed on the drill platform. The harder a layer is, the slower and more difficult it is to penetrate. Rate of penetration is also affected by a number of other factors, however, so it cannot be related directly to the hardness of the layers. Among these factors are bit weight and revolutions per minute, which are recorded on the drilling recorder.

#### Drilling Deformation

The sediment in many cores shows signs of having been disturbed since deposition. Such signs include the concave-downward appearance of originally plane bands, the haphazard mixing of lumps of different lithologies, and the near-fluid state of some sediments recovered from tens or hundreds of meters below the seafloor. It seems reasonable to assume that some of this deformation has come about during or after the cutting of the core. The processes of cutting, core retrieval (which is accompanied by changes in pressure and temperature), and core handling on board ship may all stress a core sufficiently to alter its physical characteristics.

#### Variable Length Hydraulic Piston Corer

In December 1978, The Deep Sea Drilling Project deployed the first hydraulically actuated wireline piston corer (the hydraulic piston corer or HPC). In this coring system, which is described by Prell et al. (1982), fluid pumped through the drill pipe activates a piston-driven core barrel, which is ejected through the core bit into the sediment at the rate of approximately 60 m/s. This extremely high penetration rate is independent of the motion of the drill string. After each coring operation, the core barrel assembly is retrieved by wireline, as in a conventional coring operation. The core bit is then "washed down" to the next coring point, where the piston coring procedure is repeated. Piston coring must be discontinued when the sediments become too indurated.

<sup>1</sup> Graciansky, P. C. de, Poag, C. W., et al., *Init. Repts. DSDP*, 80: Washington (U.S. Govt. Printing Office).

<sup>2</sup> Addresses: (Poag) U.S. Geological Survey, Woods Hole, Massachusetts 02543; (Foss) Scripps Institution of Oceanography, La Jolla, California 92093.

During Leg 80, an improved coring system, referred to as the variable length hydraulic piston corer (VLHPC), was used (Fig. 1). The VLHPC is capable of recovering cores up to 9.5 m in length, whereas the HPC could recover cores of 4.5 m only. The VLHPC recovers core in a standard (6.6-cm-inner-diameter) butyrate core liner. It uses a special roller cone core bit with an outer diameter of 11.5 in. and a core throat of 3.62 in.

### SHIPBOARD SCIENTIFIC PROCEDURES

#### Numbering of Sites, Holes, Cores, Sections, and Samples

DSDP drill sites are numbered consecutively from the first site drilled by *Glomar Challenger* in 1968. Site and hole numbers mean slightly different things. A site num-

ber refers to one or more holes drilled while the ship is positioned over one acoustic beacon. The holes may be anywhere within a radius of 900 m of the beacon. Several holes may be drilled at a single site by pulling the drill pipe above the seafloor (out of one hole), moving the ship 100 m or more, and then drilling another hole.

A letter suffix distinguishes additional holes drilled at the same site. The first hole takes the site number; the second takes the site number with suffix A; the third takes the site number with suffix B, and so forth. For sampling purposes it is important to specify the hole number, because sediments or rocks recovered from a given depth at different holes usually do not come from the same position in the stratigraphic column.

The cored interval is measured in meters below the seafloor. The depth interval for an individual core is the

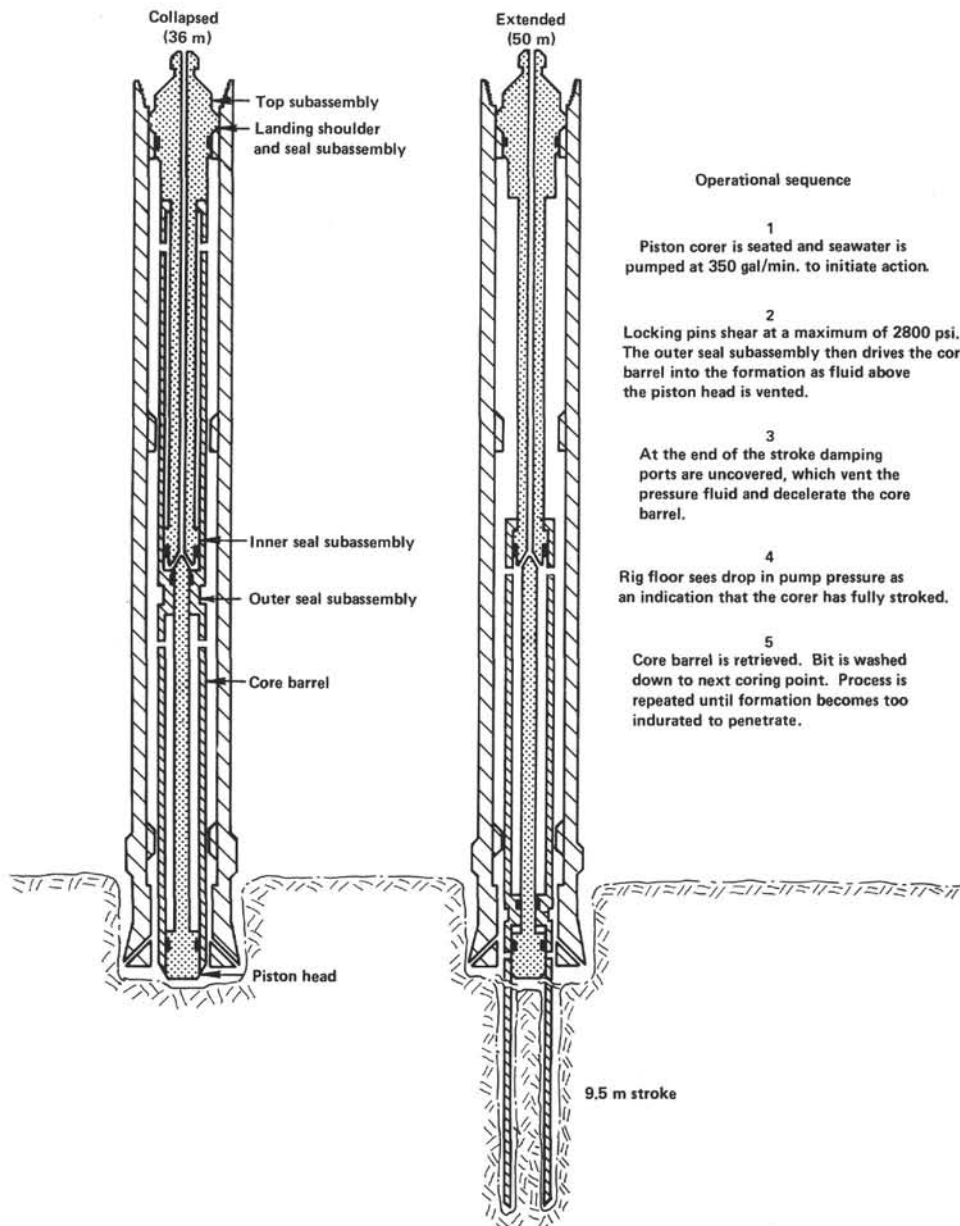


Figure 1. Variable length hydraulic piston corer.

depth below seafloor where the coring operation begins to the depth where the coring operation ends. Most coring intervals are 9.5 m long, which is the nominal length of a core barrel; however, it may be shorter. "Cored intervals" are not necessarily adjacent to each other, but may be separated by "drilled intervals." In soft sediment, the drill string can be "washed ahead" with the core barrel in place, but not recovering sediment, by pumping water down the pipe at high pressure to wash the sediment out of the way of the bit and up the space between the drill pipe and the wall of the hole.

Cores taken from a hole are numbered serially from the top of the hole downward. Full recovery for a single core is normally 9.28 m of sediment or rock in a plastic liner (6.6 cm inner diameter), plus about a 0.2-m sample (without a plastic liner) in the core catcher. The core catcher is a device at the bottom of the core barrel; it prevents the core from sliding out when the barrel is being retrieved from the hole. The sediment core, which is in the plastic liner, is cut into 1.5-m sections and numbered serially from the top of the sediment core (Fig. 2). When full recovery is obtained, the sections are numbered from 1 through 7, the deepest section possibly being shorter than 1.5 m. The core-catcher sample is placed below the last section when the core is described and labeled core catcher (CC); it is treated as a separate section.

When recovery is less than 100%, the 1.5-m sections are still numbered serially, starting with Section 1 at the top. There will be as many sections as are needed to accommodate the length of the core recovered (Fig. 2); for example, 3 m of core sample in plastic liners will be divided into two 1.5-m sections. The last section may be shorter than the normal 1.5 m.

When recovery is less than 100%, the original stratigraphic position of the sediment in the cored interval is unknown; therefore, for convenience in data handling and consistency, we arbitrarily assign the top of the recovered sediment the depth of the top of the cored interval. If recovery is less than 100%, if the core is fragmented, and if the shipboard scientists believe that the fragments were not originally contiguous, the sections are numbered serially and the intervening sections are noted as void, whether there was a space between such fragments in the core liner or not.

Samples are designated by distances in centimeters from the top of each section to the top and bottom of the sample in that section. A full identification number for a sample consists of the following information: leg, hole, core, section, and interval in centimeters. For example, the sample identification number "80-548A-30-3, 98-100 cm" means that a sample was taken between 98 and 100 cm from the top of Section 3 of Core 30, from the second hole drilled at Site 548 during Leg 80. A sample from the core catcher of this core would be designated "80-548A-30,CC, 8-9 cm."

The depth below the seafloor for a sample numbered "80-548A-30-3, 98-100 cm" is the sum of the depth to the top of the cored interval for Core 30 (481.0 m) and the 3 m included in Sections 1 and 2 (each 1.5 m long) and the 98 cm below the top of Section 3. The sample in

question is located at 484.98 m sub-bottom, which in principle is the sample depth below the seafloor (sample requests should refer to a specific interval within a core section, rather than the depth below seafloor).

Conventions regarding the cataloging of the cores recovered by the VLHPC are the same as those for rotary cores.

### Handling of Cores

A core is normally cut into 1.5-m sections, sealed, and labeled on the rig floor; the sections are then taken into the shipboard core laboratory for processing. The following determinations are normally made before the sections are split: gas analysis, thermal-conductivity analysis (soft sediment only), and continuous wet-bulk density determinations using the Gamma Ray Attenuation Porosity Evaluator (GRAPE).

The cores are then split longitudinally into working and archive halves, either by wire cutter or by rock saw. The difference in appearance between cores cut by the two methods can be striking. Samples are extracted from the working half for the measurement of sonic velocity (by the Hamilton Frame method), wet-bulk density (by a GRAPE technique), carbon-carbonate content, and carbonate content (by carbonate bomb) and for geochemical analysis, paleontologic studies, and studies of other types. When the sediments are sufficiently firm, the cut surface of the archive half is washed to emphasize sedimentary features. The color, texture, structure, and composition of the various lithologies within a section are described on standard visual core description forms (one per section), and any unusual features are noted. Finally, the archive half of the core is photographed.

After the cores are sampled and described, they are maintained in cold storage on board *Glomar Challenger* until they are transferred to the DSDP repository. Sections to be used for organic-geochemistry studies are frozen immediately on board ship and kept frozen. All Leg 80 cores, including frozen cores, are presently stored at the DSDP East Coast Repository (Lamont-Doherty Geological Observatory).

The visual examination, smear slide analyses, and carbonate-bomb (percent  $\text{CaCO}_3$ ) analyses of the cores, all of which are done on board ship, provide the data for the core description forms shown in this volume. The forms also show sample locations. A blank form is shown in Figure 3.

### Sediment and Sedimentary Rock Core Description Forms

#### Drilling Disturbance

Recovered rocks, particularly soft sediments, may be extremely disturbed. This mechanical disturbance is especially pronounced when rotary coring is used, which uses a bit 25 cm in diameter with a 6-cm-diameter opening for the core sample. The symbols for the six disturbance categories used for soft and firm sediments are shown in the "Drilling Disturbance" column in the core description form (Fig. 3). The disturbance categories are

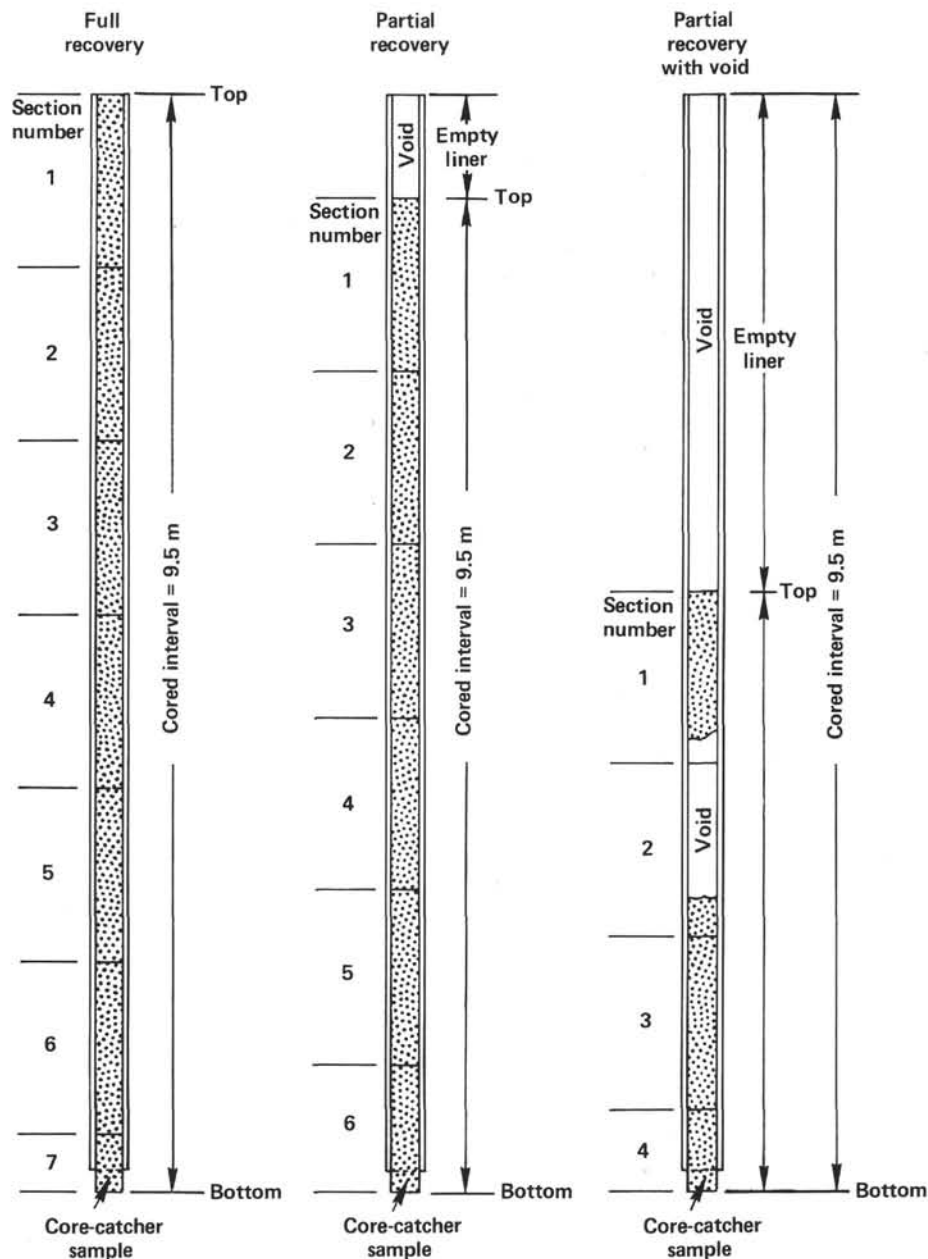


Figure 2. Core cutting and labeling procedure.

defined as follows: (1) slightly deformed—bedding contacts are slightly bent; (2) moderately deformed—bedding contacts have undergone extreme bowing, and firm sediment is fractured; (3) very deformed—bedding is completely disturbed or homogenized by drilling, sometimes showing symmetrical diapirlike structure; (4) soupy—water-saturated intervals have lost all aspects of original bedding; (5) biscuited—sediment is firm and broken into chunks 5 to 10 cm long; and (6) brecciated—indurated sediment is broken into angular fragments by the drilling process, perhaps along preexisting fractures.

#### Sedimentary Structures

In soft, and even in some harder, sediments, it may be extremely difficult to distinguish between natural structures and structures created by the coring process, and

in these instances the description of sedimentary structures is optional. The locations and types of structures are shown by graphic symbols in the "Sedimentary Structures" column in the core description form (Fig. 3). Figure 4 gives the key for these symbols.

#### Color

Colors of the core samples are determined by comparison with the Geological Society of America Rock-Color Chart (*Munsell Soil Color Charts*, 1971). Colors were determined immediately after the cores were split and while they were still wet.

#### Lithology

Lithologies are shown in the core description form by one or more of the symbols shown in Figure 5. The sym-

SITE		HOLE				CORE		CORED INTERVAL			
TIME - ROCK UNIT	BIOSTRATIGRAPHIC ZONE	FOSSIL CHARACTER				SECTION	METERS	GRAPHIC LITHOLOGY	DRILLING DISTURBANCE	SEDIMENTARY STRUCTURES	SAMPLES
		FORAMINIFERS	NANNOFOSSILS	RADIOLARIANS	DIATOMS						
	D = Diatom					1					
	R = Radiolarian					2	IW				
	F = Foraminifer					3					
						4					
						5	pp				
	N = Nannofossil					6	OG				
						7					
						CC					

Abundance:  
 A = Abundant  
 C = Common  
 F = Few  
 R = Rare  
 B = Barren

Preservation:  
 G = Good  
 M = Moderate  
 P = Poor

See key to graphic lithology symbols (Fig. 5).

See key to symbols in Figure 4.

\* = Smear slide samples

← Interstitial water sample

← Physical properties sample

← Organic geochemistry sample

← Core catcher

Lithologic description

Smear slide summary:  
 Section-interval (cm)  
 D = Dominant lithology, M = Minor lithology  
 Texture: %  
 Composition: %

Physical properties:  
 Section-interval (cm)

Carbonate bomb:  
 Section-interval (cm) = %

Figure 3. Form used to describe sediment cores (barrel sheet).

Recommended symbol	Description
	Microcross-laminae (including climbing ripples)
	Parallel bedding/laminations
	Filled fractures, veins
	Cross-stratification
	Slump blocks or slump folds
	Load casts
	Scour
	Normal graded bedding
	Reversed graded bedding
	Convolute and contorted bedding
	Sharp contact
	Scoured, sharp contact
	Gradational contact
	Fining-upward sequence
	Coarsening-upward sequence
	Interval over which a specific structure occurs in core
	Bioturbation—minor (0–30% surface area)
	Bioturbation—moderate (30–60% surface area)
	Bioturbation—strong (more than 60% of surface area)
	Microfaults (healed)
	<i>Inoceramus</i> valves
	Prominent burrows
	Flasers

Figure 4. Symbols used to show sedimentary structures in sediment core description forms.

bols in a group, such as CB, correspond to end-members of sediment compositional range, such as nannofossil ooze or nannofossil chalk/marl. The symbol for the terrigenous constituent appears on the right side of the column, the symbol for the biogenic constituent(s) on the left side of the column. The abundance of any component approximately equals the percentage of the

width of the graphic column its symbol occupies. For example, the left 20% of the column may have a diatom ooze symbol, whereas the right 80% may have a silty clay symbol, indicating sediment composed of 80% silty clay and 20% diatoms.

Because of the difference in the length-to-width ratio between the actual sediment core and the graphic lithologic column it is not possible to reproduce structures as they appeared in the core; in the graphic representation they are highly flattened and distorted. The same is true for rock fragments or pebbles in the cores.

Smear-slide (or thin-section) compositions, carbonate contents (percent CaCO<sub>3</sub>), and organic carbon contents determined on board are listed below the core description; the two numbers separated by a hyphen refer to the section and centimeter interval, respectively, of the sample. The locations of these sample in the core and a key to the codes used to identify these samples are given in the "Samples" column (Fig. 3). The locations and intervals of the organic geochemistry, interstitial water, and physical property samples are given in the lithologic column.

### Lithologic Classification of Sediments

The basic classification system used here was devised by the JOIDES Panel on Sedimentary Petrology and Physical Properties and adopted for use by the JOIDES Planning Committee in March 1974. This classification is descriptive rather than generic, and divisions between different types of sediment (Fig. 6) are somewhat arbitrary. We treat lithologic types not covered in this classification as a separate category termed Special Rock Types. A brief outline of the conventions and descriptive data used to construct this classification follows.

### Composition and Texture

In this classification, composition and texture are the only criteria used to define the type of sediment or sedimentary rock. Composition is more important for describing sediments deposited in the open ocean, and texture becomes significant for hemipelagic and nearshore sediments. These data come principally from the visual analysis of smear slides with a petrographic microscope. The data are estimates of the abundance and size of the components on a slide and may differ somewhat from the results of more accurate shore-based analyses of grain size, carbonate content, and mineralogy. Past experience indicates that quantitative estimates of distinctive minor components are accurate within 1 to 2%, but that accuracy for major constituents is poorer ( $\pm 10\%$ ). All smear slide estimates were made on board.

When appropriate, modifiers are used to name the type of sediment encountered. In all cases the dominant component appears last in the name; minor components precede, with the least common constituent listed first. Minor constituents occurring in amounts less than 10% are not included in the name. This convention also holds for zeolites, iron and manganese-micronodules, and other indicators of very low rates of sedimentation or non-deposition, such as fish teeth. Often these minerals are conspicuous, even though greatly diluted. If deemed im-

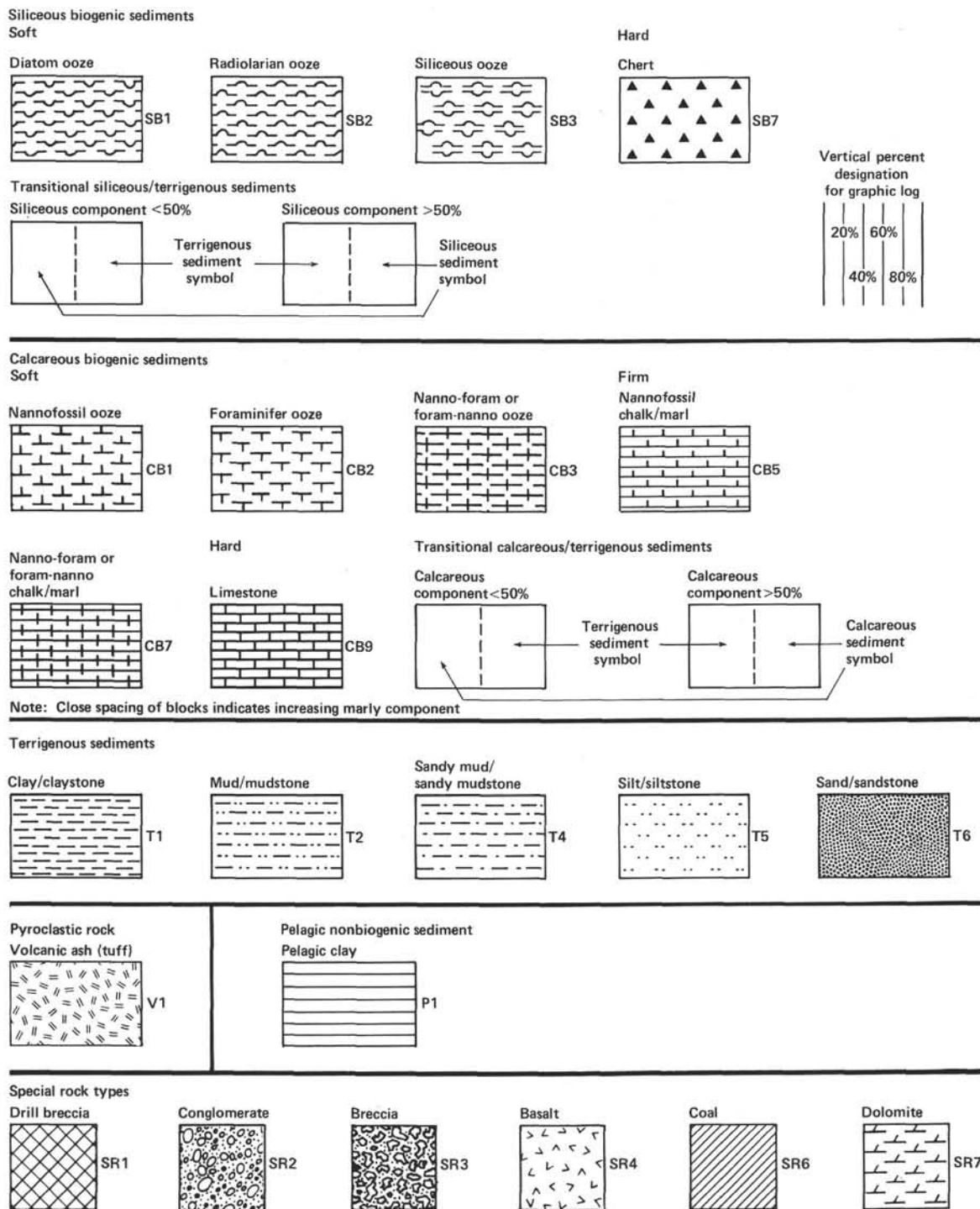


Figure 5. Symbols used in graphic lithology columns of sediment core description forms.

portant, they are sometimes included in the name of the sediment or mentioned in the lithologic description.

**Induration of Sediments**

We recognize three classes of induration or lithification for all sediments. For calcareous sediments and sedimentary rocks (categories after Gealy et al., 1971), (1) soft = ooze; has little strength and is readily deformed

under pressure of finger or broad blade of spatula; (2) firm = chalk; partially lithified, readily scratched with fingernail or edge of spatula; (3) hard = limestone, dolostone, well lithified and cemented, resistant or impossible to scratch with fingernail or edge of spatula. For transitional carbonates and siliceous, pelagic, and terrigenous sediments, the three classes of induration are as follows: (1) soft = sediment core may be split with

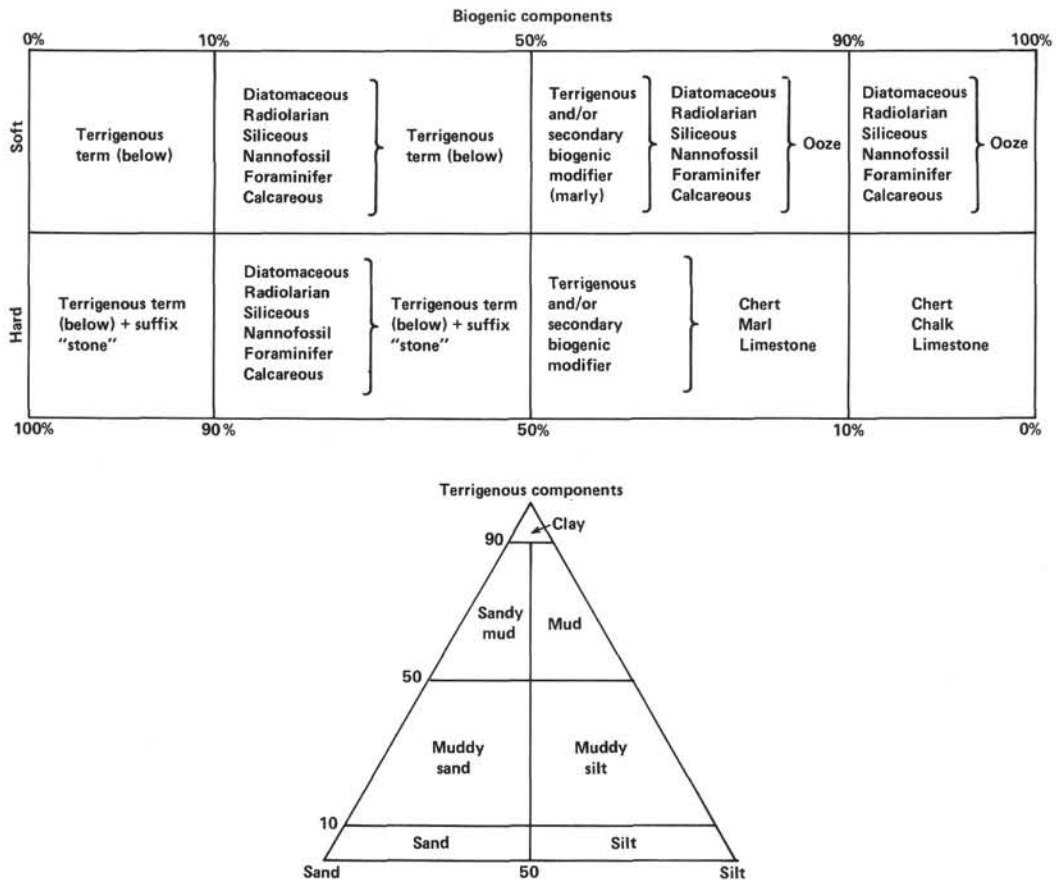


Figure 6. Textural classification of clastic sediments.

wire cutter; (2) firm = partially lithified but fingertip pressure leaves an indentation; (3) hard = cannot be compressed with fingertip pressure.

**Types of Sediment and Sedimentary Rocks, Compositional Boundaries**

**Pelagic Clay**

Pelagic clay is principally an authigenic deposit that accumulates at very slow rates. The class has also often been termed brown clay or red clay.

The boundary between pelagic clay and terrigenous sediment occurs where authigenic components (Fe/Mn micronodules, zeolites), fish debris, and other microfossil constituents reach 10% in smear slides, greater percentages indicating pelagic clay. Because the accumulation rates of pelagic clay and terrigenous sediments are very different, transitional deposits are exceptional.

The boundary between pelagic clay and siliceous biogenic sediment occurs where siliceous remains make up 30% of the content.

The boundary between pelagic clay and calcareous biogenic sediment occurs where the biogenic CaCO<sub>3</sub> content of the sediment exceeds 30%. However, the mixture of pelagic clay and calcareous biogenic sediment is uncommon. Generally pelagic clay passes through siliceous ooze to calcareous ooze, with one important ex-

ception: at the base of many oceanic sections, black, brown, or red clays lie directly on basalt, and they are overlain by or grade up into calcareous sediments. Most of the basal clayey sediments are rich in iron, manganese, and other metallic trace elements.

**Pelagic Siliceous Biogenic Sediment**

Pelagic siliceous biogenic sediment is distinguished from pelagic clay by having more than 30% siliceous microfossils. Siliceous biogenic sediments are distinguished from calcareous biogenic sediments by having a calcium carbonate content of less than 30%.

For a pelagic biogenic siliceous sediment with 30 to 100% siliceous fossils, the following terminology is used. Soft denotes siliceous ooze (radiolarian ooze or diatomaceous ooze, depending on the dominant fossil component), and hard denotes radiolarite, diatomite, chert, or porcellanite. Diatoms and radiolaria may also be used as compositional qualifiers, separately or together. The order of the two are qualifiers, if they are used together, depends on the dominant fossil type. The dominant component is listed last and the minor component first.

**Pelagic Biogenic Calcareous Sediment**

Pelagic calcareous sediment is distinguished from pelagic clay by having a biogenic CaCO<sub>3</sub> content in excess of 30%. There are two classes: pelagic biogenic calcare-

ous sediments that contain 60 to 100% biogenic  $\text{CaCO}_3$  and transitional biogenic calcareous sediments that contain 30 to 60%  $\text{CaCO}_3$ .

For the pelagic biogenic calcareous sediment with 60 to 100%  $\text{CaCO}_3$ , the following terminology is used: calcareous ooze for soft sediments; chalk for firm sediments; and limestone for hard and cemented sediments. Compositional qualifiers are also used (if nannofossils and foraminifers are the principal components, either or both may be used).

The transitional biogenic calcareous sediments with 30 to 60%  $\text{CaCO}_3$  are termed marl or marlstone, depending on whether they are soft or hard.

#### **Terrigenous Sediment**

Terrigenous sediments are distinguished from pelagic sediments by having a terrigenous component in excess of 30% and siliceous and authigenic (pelagic) components each less than 10%. Sediments in this category are subdivided into textural groups by smear slide estimates or grain-size analyses of the relative proportions of sand, silt, and clay. The grain-size limits are those defined by Wentworth (1922). Textural classification follows the triangular diagram (Fig. 6).

#### **Hemipelagic Sediment**

Sediments transitional between pelagic and terrigenous sediments are termed hemipelagic. These sediments are characterized by a terrigenous component in excess of 30%, a total nonbiogenic component in excess of 40%, and a biogenic content in excess of 10%. In addition to having a comparatively large terrigenous component, hemipelagic sediments may be rich in biogenic silica (usually diatoms, because of coastal upwelling) and volcanic ash (predominantly along active margins).

#### **Volcanogenic Sediment**

Pyroclastic rocks are described according to the textural and compositional scheme of Wentworth and Williams (1932). The textural groups are as follows: fragments of more than 32 mm are termed volcanic breccia; fragments of 32 to 4 mm are termed volcanic lapilli; and particles less than 4 mm are termed volcanic ash (tuff when indurated). The composition of these pyroclastic rocks is described as vitric (glass), crystalline, or lithic.

Sediments rich in ash are described in the following manner:

Ash (%)	Soft sediment	Indurated
0-10	Mud	Mudstone
10-30	Vitric mud	Vitric mudstone
30-60	Muddy ash	Tuffite
>60	Ash	Tuff

#### **Special Sedimentary Rock Types**

The definition of and nomenclature for sediment and rock types not included in the system described above are left to the discretion of shipboard scientists, with the

recommendation that they adhere as closely as possible to conventional terminology. This category includes such rocks as evaporites (halite, anhydrite, and gypsum); shallow-water limestone (biostromal, biohermal, coquina, and oolite); dolomite; and gravels, conglomerates, and breccias.

#### **Qualifiers**

In general, substances that make up 10 to 30% of the sediments may be identified in the name of sediment (e.g., vitric diatomaceous mud or vitric muddy diatomaceous ooze). If more than one such qualifier is used, they are listed in order of increasing abundance in the sediment.

#### **Biostratigraphy and Basis for Age Determination**

Several biozonations were used for the various microfossil groups found in the Leg 80 sedimentary rocks. The basic biostratigraphic framework for the Cretaceous has been provided by Müller (this volume), who incorporated information from Martini (1976), Čepok and Hay (1969), and Bukry and Bramlette (1970) into the nannofossil zonations of Thierstein (1973, 1976); and Magniez and Sigal (this volume), who used the foraminiferal subdivisions of Bettenstaedt (1952), Bartenstein (1978), and Sigal (1977). The biostratigraphic framework for the Cenozoic is based on Müller (this volume), who used the standard nannofossil zonation of Martini (1971); and Snyder and Waters (this volume), who incorporated information from Stainforth et al. (1975) and Poore (1979) into the planktonic foraminifer zonal schemes of Blow (1969) and Berggren and Van Couvering (1974).

Where possible, paleomagnetic interpretations (Townsend, this volume) are correlated with biostratigraphic subdivisions. Unfortunately, at several sites no conclusive magnetic polarity sequence could be defined for large portions of the sedimentary section. In Hole 549A, for example, all the sediments below the base of the Pleistocene (27 m below seafloor) are weakly magnetized. Because interpretations must, therefore, be based solely on natural remanent magnetizations (NRM), the magnetostratigraphy is tentative. Elsewhere, the combination of poor core recovery, sediment condensation, and the frequency of the reversals make the magnetostratigraphy difficult to interpret (e.g., the Miocene section of Hole 550).

At the time of this writing, Berggren et al. (in press) are compiling first-order biostratigraphic datum levels against magnetic stratigraphy in order to update the Cenozoic time scale. This compilation is likely to change the absolute ages of some magneto- and biostratigraphic events. For example, previous correlations between biostratigraphy and age estimates for the lower/middle Eocene boundary are probably incorrect (Berggren, pers. comm., 1982). For the site chapters, we have not proposed new correlations among biostratigraphy, magnetostratigraphy, geochronology, and absolute dating, but have simply adopted the absolute ages suggested by Hailwood et al. (1979), with the full understanding that some modifications are imminent. This approach pro-

vides a frame of reference for the interpretation of our data. It also simplifies comparisons with results from Leg 48 (Bay of Biscay).

### Paleoenvironmental Interpretations

Paleoenvironmental conditions of sedimentary sections are generally interpreted in terms of seafloor conditions during deposition. Thus terms such as *inner* or *outer sublittoral* are used rather than *inner* or *outer neritic*, which refer to conditions in the water column. In general, benthic organisms are used for seafloor environmental interpretations and planktonic organisms are used to detect paleoceanographic and paleoclimatic signals originating in the water column.

### Shipboard Geochemical Measurements

#### Carbonate Bomb

Percent  $\text{CaCO}_3$  was determined on board ship by the "Karbonate Bombe" technique (Müller and Gastner, 1971). In this simple procedure, a sample is ground to powder and treated with HCl in a closed cylinder. Any resulting  $\text{CO}_2$  pressure is proportional to the  $\text{CaCO}_3$  content of the sample. The application of a calibration factor to the manometer reading ( $\times 100$ ) yields percent  $\text{CaCO}_3$ . Percent error can be as low as 1% for sediments high in  $\text{CaCO}_3$ , and an overall accuracy of 2 to 5% can be obtained.

These data are presented in the core-description forms (Fig. 3). The sample interval is designated by two numbers: the section number, followed by the top of the sample interval. For example, a sample from Section 2, 11 to 12 cm, with 90% calcium carbonate will be represented on the core description sheet as "2-11 (90%)."

#### Rock-Eval Pyrolysis

Pyrolysis of sediments using a Girdel Rock-Eval apparatus yielded information on the amount, type, and thermal maturity of the organic matter in the Leg 80 samples (Espitalié et al., 1977). The Rock-Eval technique involves heating a powdered 100-mg rock sample from 250°C to 550°C at the rate of 25°C/min. At the beginning of this heating program, volatile organic compounds (free hydrocarbons) indigenous to the sample are liberated and measured by a flame ionization detector (FID). The quantity measured is known as  $S_1$ . Further into the heating program the heat cracks the kerogen in the rock sample. The hydrocarbons thus produced are measured by the FID and are known as  $S_2$ , the hydrocarbon-generating potential of the sample. At the same time as  $S_1$  is being liberated and  $S_2$  is being generated,  $\text{CO}_2$  is being produced from the organic matter. It is trapped until the pyrolysis temperature reaches 390°C. This  $\text{CO}_2$  is then released at the end of the analysis, when it is measured by a thermal conductivity detector. The  $\text{CO}_2$  peak is known as  $S_3$ . The quantities  $S_1$  and  $S_2$  are typically expressed in milligrams of hydrocarbon per gram of rock, while  $S_3$  is expressed as milligrams of  $\text{CO}_2$  per gram of rock.

The  $S_2$  value may be used as an indication of the hydrocarbon source potential. The  $S_2/S_3$  ratio is an indication of the expected type of hydrocarbon generated (gas

vs. oil). The  $S_1/S_1 + S_2$  ratio is an indication of the production potential (Clementz et al., 1979). In addition, the temperature of maximum pyrolysis yield ( $T_{\text{max}}$ ) may be used as an indication of organic maturity.

### Other Geochemical Analyses

Shipboard analyses of the sediment for carbon-carbonate, pH, alkalinity, salinity, calcium, magnesium, and chlorinity are conducted routinely. A limited number of carbon-carbonate analyses are made using a LECO WR-12 Carbon Analyzer. Sample preparation includes the drying, grinding (with a Diamonite mortar and pestle), and weighing out of two 0.1 g samples. One of these is analyzed for total carbon after being wetted with deionized water and dried. The other is analyzed for organic carbon after being acidified to remove acid-soluble components and dried. Reproducibility tests are not run, but the accuracy of the total carbon and organic carbon analyses should be near  $\pm 4\%$  (relative) and that of the carbonate analysis should be about  $\pm 2\%$  (absolute).

Interstitial waters are routinely analyzed for pH, alkalinity, salinity, calcium, magnesium, and chlorinity. Sediments are squeezed in a stainless steel press; the water is collected in plastic syringes and is then filtered through 0.45- $\mu\text{m}$ , 1-in.-diameter millipore filters. Interstitial waters collected with the *in situ* water sampler are filtered through 0.4- $\mu\text{m}$ , 13-mm-diameter filters before being analyzed.

A Corning Model 130 pH meter and a Markson combination electrode were used to determine pH. The pH meter is calibrated with 4.01 and 7.42 buffer standards; all readings are originally in millivolts and converted to pH later. All pH measurements are made in conjunction with alkalinity measurements.

Alkalinities are determined potentiometrically. The samples (5–10 ml in volume) are first tested for pH and then titrated with 0.1 N HCl. Near the endpoint, acid is added in 0.01-ml or 0.005-ml increments, and the millivolt readings are noted for each increment. The exact endpoint is then calculated by the Gran Factor method (Gieskes and Rogers, 1973).

Salinity is calculated from the fluid refractive index, as measured by a Goldberg optical refractometer, by using this expression:

$$\text{Salinity (\%)} = 0.55 \times \Delta N,$$

where  $\Delta N$  is the refractive index multiplied by  $10^4$ . The refractometer's calibration is checked periodically by using IAPSO standard seawater and deionized water.

Calcium is determined by titrating a 0.5-ml sample with EGTA (a complexing agent); GHA is used as an indicator. To sharpen the endpoint, the calcium-GHA complex is extracted into a layer of butanol. No correction is made for strontium, which is also included in the result.

Magnesium is determined by titrating a buffered 0.5-ml sample to an Eriochrome Black-T endpoint, using EDTA (sodium salt) as a titrant. This method analyzes all alkaline earths, including calcium, magnesium, strontium, and magnesium; concentrations are obtained by

subtracting the calcium (which includes strontium) from this analysis.

Chlorinity is determined by titrating a 0.1-ml sample diluted with 1 ml of deionized water with silver nitrate to a potassium chromate endpoint.

Methods and equipment are checked and standardized at each site using IAPSO standard seawater. As a further check, a surface seawater sample is also analyzed and archived. This sample is also used to test for the contamination of the interstitial water samples by drill water.

### Physical Properties—Measurement Procedures

A thorough discussion of measurement procedures for physical properties, including descriptions of equipment, methods, errors, correction factors, and problems related to coring disturbance, is presented by Boyce (1976). Only a brief review of the methods employed on Leg 80 is given here.

#### Sonic Velocity

Compressional-wave velocities were measured on the Hamilton Frame Velocimeter by timing a 400-kHz pulse between two transducers and by measuring the distance across the sample with a dial gauge. For unconsolidated sediments, velocities were generally measured on the split core; correction factors established by Boyce (1976) were used to compensate for the increase in thickness and travel time due to the polycarbonate liner (0.242 cm and 1.108  $\mu$ s, respectively). For consolidated sediments, a piece removed from the core was tested. The piece was trimmed carefully to form two parallel surfaces to ensure good contact with the transducer heads. Salt water was used to make an acoustic contact between the sample and the transducers.

Calibration measurements were made with a lucite standard with an assumed velocity of 2.745 mm/ $\mu$ s and a length of 31.84 mm. The corresponding calculated travel time was 11.60  $\mu$ s. Twenty measurements were made with a Tektronix 485 oscilloscope, and thickness measurements of the lucite standard were made with a dial gauge integral to the Hamilton Frame. The average length was 31.74 mm, approximately 0.04 mm less than expected. The observed average travel time was 11.596  $\pm$  0.073 s. The calculated lucite velocity was 2.735  $\pm$  0.018 mm/ $\mu$ s. The accuracy of the Hamilton Frame velocity device was 0.4%, which can be stated as 0.7% precision. A calibration constant, or correction factor, was not used on shipboard velocity measurements.

#### GRAPE

The Gamma Ray Attenuation and Porosity Evaluator (GRAPE) was used to determine wet-bulk density. The determination is based on the attenuation of gamma rays that are sent through a sample. Boyce (1976) discusses the theoretical aspects of this method in detail. During Leg 80, the GRAPE was used in two modes: (1) continuous GRAPE, in which most sections of the core were irradiated, and continuous "corrected" wet-bulk density (relative to quartz) was plotted on an analog

graph; and (2) 2-minute GRAPE, in which the gamma ray count through a small piece of the core was measured for 2 minutes. A similar count through air and/or a quartz standard followed.

#### Continuous GRAPE

Before each core was run through the device, an aluminum standard was measured. An equivalent density of 2.60 Mg/m<sup>3</sup> was assigned to the 6.61-cm (diameter) aluminum standard analog record, and a density of 1.0 Mg/m<sup>3</sup> was assigned to the 2.54-cm (diameter) aluminum standard analog record. Linear interpolation of the GRAPE analog data between these values yields an "empirical" wet-bulk density of the sediment sample in the core ( $\rho_{bcz}$ ). If the sediment completely fills the core, then  $\rho_{bc}$  = "corrected" wet-bulk density (relative to quartz). Then:

$$\rho_b = \frac{(\rho_{bc} - \rho_{fc})(\rho_g - \rho_f)}{(\rho_{gc} - \rho_f)} + \rho_f,$$

where  $\rho_b$  = true wet-bulk density;  $\rho_{fc}$  = salt-corrected fluid density ( $\sim$  1.128 Mg/m<sup>3</sup>);  $\rho_g$  = true grain density ( $\sim$  2.71 Mg/m<sup>3</sup> for calcareous sediments, and  $\sim$  2.80 Mg/m<sup>3</sup> for terrigenous clays; Mitchell, 1976);  $\rho_f$  = true fluid density ( $\sim$  1.025 Mg/m<sup>3</sup>);  $\rho_{gc}$  = salt-corrected grain density (assumed equal to  $\rho_g$ ).

If the above values for calcareous sediments are used,

$$\rho_b = 1.065 (\rho_{bc} - 1.128) + 1.025;$$

for terrigenous clay deposits,

$$\rho_b = 1.062 (\rho_{bc} - 1.128) + 1.025.$$

The porosity  $\phi$  is obtained by using the equation

$$\phi(\%) = \frac{\rho_g - \rho_b}{\rho_g - \rho_f} \times 100.$$

No corrections are made for core samples that did not fill the liner.

#### Two-Minute GRAPE

For 2-minute GRAPE calculations,

$$\rho_{bc} = \frac{\ln(I_0/I)}{d \mu_{qtz}},$$

where  $I_0$  = 2-minute gamma count through air,  $I$  = 2-minute gamma count through the sample,  $d$  = gamma ray path length through the sample, and  $\mu_{qtz}$  = quartz attenuation coefficient determined daily by measuring through a quartz standard. Then, as in the continuous GRAPE calculation (assuming a 2.71 grain density),

$$\rho_b = 1.066 (\rho_{bc} - 1.128) + 1.025$$

and

$$\phi(\%) = \frac{100(2.71 - \rho_b)}{1.685}$$

Boyce (1976) estimates  $\pm 5\%$  accuracy for continuous GRAPE data and  $\pm 2\%$  for 2-minute GRAPE data. In practice, the error seemed to be higher, probably partly because of core disturbance and partly because swelling in the sediments caused errors in the determinations of gamma ray travel paths. However, agreement is good (within the accuracies estimated by Boyce) between the GRAPE data from selected portions of nearly every section and the results of gravimetric analysis.

#### Gravimetric Analysis

In a soft sediment (one recovered from less than 150 m sub-bottom), a 1-cm<sup>3</sup> syringe was used to collect a measured volume of sediment for shipboard analysis. In harder sediments, a 10 to 30 cm<sup>3</sup> chunk of rock was analyzed. A small piece of this chunk was used for water content determination only; the remainder was used for a volume determination by immersion in water. Wet-bulk density, porosity, grain density, and water content were then determined. No corrections for salt were made in any of these calculations.

$$100 \times \frac{\text{Water content (\% wet wt.)} = (\text{wt. wet sediment}) - (\text{wt. dry sediment})}{(\text{wt. wet sediment})}$$

and

$$\text{wet-bulk density (Mg/m}^3\text{)} = \frac{\text{wt. wet sediment}}{\text{vol. wet sediment}}$$

The 1-cm<sup>3</sup> syringe samples provide volume measurements. Bennett and Keller (1973) note, however, that the volumes are too small for an accurate determination of grain density or porosity. Accuracy may also be adversely affected by slight errors in sampling techniques; any cracks or voids in the sample lead to large inaccuracies. In addition, despite all precautions, almost all samples are affected by some compression, which leads to inaccuracies in the volume measurements. Large samples taken for shore-based determinations provide more accurate results.

For the syringe and rock chunk samples, porosity is computed as follows:

$$\text{Porosity (\%)} = 100 \times \frac{\text{wt. evaporated water}}{\text{vol. wet sediment}}$$

In general, the results of the gravimetric analyses can be compared with the GRAPE data. When good sampling techniques are followed (and good samples are available), the data generally agree well. Statistical analysis shows that the 2-minute GRAPE wet-bulk densities are 2% higher than the gravimetric measurements. No large-diameter syringe samples were obtained because the necessary equipment was not available.

#### Shear Strength Measurements

A CL-600 Torvane Soiltest Pocket Penetrometer and a Wykeham Farrance vane apparatus were used on board to determine the undrained shear strength of both clayey and calcareous sediments obtained by hydraulic piston coring. The Torvane penetrometer is hand rotated at a rate designed to cause the sediments to reach failure in about 10 s with constant loading. Repeated determinations yielded results that were generally reproducible to  $\pm 10\%$ . Measurements were made in the least disturbed sections of the split core, parallel to the core axis, and were discontinued when cracking of the sediments was observed, indicating failure by fracturing instead of by shear.

The penetrometer was pushed into undisturbed sections of the split core, providing unconfined compression strength,  $q_c$ . Shear strength was related to compression strength by Terzaghi and Peck (1967):

$$\tau_p = q_c/2,$$

where  $\tau_p$  = shear strength at failure.

The Wykeham Farrance vane apparatus was also used on undisturbed sections of the split core. The 1.28-cm vane was inserted 1 cm into the (half) core with the vane axis parallel to bedding and rotated by a motor at 89°/minute. Resistance springs were selected so that shearing occurred between 30 and 1.10° stress. Shear strength was calculated by Boyce (1977) as follows:

$$\tau_f = c = \frac{2t}{\pi d^2 \left(1 + \frac{2}{3h}\right)} \quad (\text{maximum degree spring stress}),$$

where  $\tau_f = c$  = cohesion and shear strength of clay at failure,  $t$  = spring torque factor in gcm/deg,  $d$  = diameter of vane blades, and  $h$  = height of vane blades.

#### Downhole Logging

Most of the downhole logging tools used for Leg 80 were the same as those used on Legs 46 to 57, except that the borehole compensated sonic log (BHC), a standard oilfield tool, was replaced by a special long-spaced sonic log (LSS). Data processing and presentation were greatly enhanced by the addition of a shipboard CYBER computer unit. See Lynch (1962) and Schlumberger (1969, 1972) for discussions of the general theory and application of the various well logs.

Successful logs were recorded at three of the four sites drilled. Hole 549 was filled with fresh water/bentonite mud for logging, whereas Holes 548A and 550B were filled with only seawater. Table 1 gives a summary of the logging operations for the leg. In addition to providing information for correlation with physical property measurements, the logs proved to be helpful to those doing lithostratigraphic work; in sections of otherwise uniform biogenic calcareous ooze, clay concentrations marking unconformities and periods of low sedimentation rates could readily be identified in the gamma ray logs.

Table 1. Downhole logging summary, Leg 80.

Hole	Total depth (m) <sup>a</sup>	Water depth (m)	Depth of open end of pipe (m)	Fluid in hole	Bit size (in.)	Logs recorded <sup>b</sup>	Depth of logged interval (m)	Observations
548	1467	1256	—	—	—	—	—	No logs requested—VLHPC hole.
548A	1807.5	1256	1429	Seawater	9 7/8	LSS-DISF-GR-CAL	1788-1428.5	Good logs—sonic velocities seem high. Wave form and variable density presentations included.
548A	1807.5	1256	1429	Seawater	9 7/8	FDC-CNL-GR-CAL	1783.5-1428.0	Caliper shifted (1 in. too big); otherwise good log. GR and CNL logged to above seafloor.
549	3534.5	2533	2642	Gel mud	9 7/8	LSS-DISF-GR-CAL	3532-2642	Sonic log poor—inadequate centralization. GR logged to above seafloor; DISF capability lost when tool was damaged (it dropped down the hole).
549A	2731.5	2535.5	—	—	—	—	—	No logs requested—VLHPC hole.
550	4968.5	4432	—	—	—	—	—	Hole aborted by weather—unable to log.
550A	4527.0	4432	—	—	—	—	—	Struck boulder at 95 m—no logs.
550B	5152.5	4432	4523	Seawater	9 7/8	LSS-GR-CAL	5123-4523	Caliper shifted; GR run to 4518 m.
550B	5152.5	4432	4523	Seawater	9 7/8	DLL-GR	5123-4523	Good log.
550B	5152.5	4432	4551	Seawater	9 7/8	FDC-CNL-CAL-GR	5123.5-4551	Caliper dead; GR run to 4528 m.
551	4110.0	3909	—	—	—	—	—	No logs requested—shallow penetration and time limitation.

<sup>a</sup> Water depth plus depth of penetration.

<sup>b</sup> LSS = long-spaced sonic; DISF = dual induction—spherically focused; GR = gamma ray; CAL = caliper; FDC = formation density; CNL = compensated neutron log; DLL = dual laterolog.

The CYBER computer unit greatly increased the usefulness of the logs to those on board ship because the digitized data on the master tapes were available to them. Previously, the tapes had to be sent ashore for processing, and only analog prints were available for shipboard work. Customer-formatted tapes are now produced as the logs are recorded, and computed logs and data cross-plots can be made on board by merging tapes from different log runs. Corrections, depth shifts, conversions, and scale changes can be made at will.

The long-spaced sonic log (LSS) determines formation velocity by measuring the time difference between the arrivals of a transmitted pulse at two receivers a known distance apart. Velocity is an important parameter in calculating porosity. The standard presentation of the data in the industry is travel time in microseconds per foot. Access to the digitized data tapes enabled the logging engineer to convert the data for Leg 80 and present velocity in kilometers per second. The geometry of the LSS permitted adequate discrimination of the weak first wave arrivals in low velocity (1.6–1.7 km/sec) sediments. Good quality logs were thus recorded in types of sediment that had yielded poor BHC logs (logs with much cycle skipping) in the past. The bed resolution of the LSS is about 60 cm.

Integrated vertical travel time is presented as a series of tick marks on the inner margin of the log. Each mark represents a 1-ms increase in total travel time. Travel time between suspected seismic reflectors can thus be determined by simply counting the marks between them.

The sonic logging equipment can also be used to record a full wave train log (on a separate run through the open hole). The successive wave arrivals are normally presented in a variable density “microseismogram” to identify such features as fractured intervals.

The dual induction—spherically focused log (DISF) measures the electrical properties of the formation at

three depths of investigation. Electrical focusing coils force high-frequency alternating current into the formation and away from the vertical borehole path. The alternating magnetic field that results from the transmitted current produces secondary electrical currents in the formation. The secondary currents, in turn, produce secondary magnetic fields that are detected by receiver coils. These coils then produce currents that are essentially proportional to the conductivity of the formation. The conductivity values are converted by reciprocation from millimhos/meter to ohm-meter for correlation with conventional resistivity log presentations. Conductivity curves that read about 1 m and 70 cm into the formation are prepared, as well as micro-spherically-focused log curve. The latter is a focused resistivity device that has been developed to investigate the formation only a few centimeters into the wall of the hole while minimizing the borehole effect.

The DISF log is a good basic log for correlation and gives excellent bed definition—down to a few centimeters. The three curves (those for 1 m, 70 cm, and several cm into the formation) give a profile of the extent of drilling fluid invasion into the formation (but only if the resistivities of the formation water and the drilling fluid are different). The extent of invasion can be an important indicator of permeability. Unlike most other electric logs, the induction log is virtually unaffected by the conductivity of the drilling fluid (i.e., seawater) in the hole. Also, since conductivity is the measured property, the measurements in highly conductive formations tend to be more accurate than those made with resistivity devices.

The dual laterolog (DLL) was deployed in Hole 550B after the dual induction tool was damaged in Hole 549. The dual laterolog, which was carried along as a backup electrical logging tool, is a combination of two focused resistivity devices (one for deep and one for shallow in-

vestigation). Data are presented as resistivity in ohm-meters on a logarithmic scale. Like the induction log, the laterolog is little influenced by the resistivity of borehole fluid and gives good bed definition. The laterolog is particularly effective in formations with high resistivity.

The formation density log (FDC) is an alternative (or a complement) to the sonic velocity and neutron porosity logs. It provides a way to determine formation porosity. The logging sonde carries a source of medium-energy gamma rays; the source is in contact with the wall of the hole. A companion detector counts back-scattered gamma rays that return to the tool as a result of the Compton scattering effect, which occurs when the gamma rays emitted by the source collide with electrons in the formation. The number of rays detected is proportional to the number of collisions, which is proportional to the number of electrons encountered—and therefore to the electron density of the formation. Electron density is related to true bulk density,  $P_b$ , in g/cc, which in turn depends on the density of the rock matrix material, the formation porosity, and the density of fluids filling the pores. The primary log trace is a linear presentation of bulk density in g/cc; porosity and  $\Delta\rho$  (correction) curves can be produced if they are desired.

The compensated neutron log (CNL) provides a porosity determination that is independent of other parameters. The device bombards the formation with high-energy neutrons from an americium-beryllium source. The neutrons that collide with hydrogen nuclei in the formation lose enough energy to slow to thermal velocities. These thermal-velocity neutrons are then counted by the detector in the sonde, with the rate of detection proportional to the concentration of elemental hydrogen in the formation. Hydrogen is found primarily in water and liquid hydrocarbons, so the porosity of the formation can be calculated from the rate at which thermal neutrons return to the sonde, with certain corrections for such factors as salinity, bound water, and matrix lithology. Free gas provides anomalously low porosity readings because of its low hydrogen density; such readings can be valuable, because they reveal the presence of gas reservoirs and the location of the *in situ* gas/liquid phase boundaries. If the formation is believed to be rock, the log can be set up to present porosity values directly. It is understood that further correction for rock type and borehole diameter might be required.

Caliper (CAL) log curves are displayed with the LSS and FDC logs. The three bow springs of the caliper used on the sonic sonde also serve to centralize for the tool in the hole. They are tied together mechanically and can expand to a maximum of only 16 in. (40.5 cm), so they can present a measurement of only the minimum diameter of the hole. Sediment tends to collect in the mechanism and can either immobilize it or cause shifts in the hole diameter curve. The single-arm caliper of the FDC log, which holds the radioactive source against the (low) side of the hole, also serves as an excentralizer. It opens only to about 12 in. (30.5 cm). Both caliper logs are useful in identifying “washed out” zones (zones where the sediment is unusually soft or friable) and in calculating hole volume for hydrogeologic, plugging, or cementing calculations.

A natural gamma ray (GR) log curve is recorded on each log run to provide a common correlation curve. The downhole tool is a simple scintillation counter that registers naturally occurring gamma radiation from radioactive isotopes (principally  $K^{40}$ ) in the formation. These radioactive elements are generally concentrated in clays, although they may also be concentrated in potassium salts, granite wash, and beds with high uranium or thorium content. Thus, the GR log is normally a reliable indicator of clay content, and it is valuable in differentiating the members of sand/shale or carbonate/shale sequences. (Other logs are necessary to differentiate the members of low-gamma radiation sequences.) By convention, the gamma ray curve is located on the left side of the log and is a linear presentation in API units, for which there are accepted industry calibration standards.

DSDP and some industry logs use the gamma ray curve as a substitute for a spontaneous potential (SP) curve. The SP curve is a recording of the potential between an electrode fixed at the drill floor and an electrode moved from the bottom to the top of the borehole. Because this “battery effect” depends upon a considerable difference in conductivity (e.g., salinity) between the borehole fluid and the formation fluid, the log is generally useless in DSDP holes drilled with seawater (even if the hole is later filled with fresh water mud for logging). As there is no extra charge or operating time involved, however, SP is normally recorded on tape during the induction or laterolog run. SP can be used to identify permeable beds, indicate clay content, or calculate formation water resistivity ( $R_w$ ). Presentation is linear and in millivolts.

## Basement Description Conventions

### Core Forms

The core description forms used for igneous and metamorphic rocks (Fig. 7) differ from those used for sediments. Igneous rock representation on these sheets is compressed, each column describing one 1.5-m section. Shipboard hand-specimen and thin-section descriptions for each section are presented at the right.

All basalts are split by rock saw into archive and working halves. The working half is described and sampled on board. In a typical basalt description form, the left box is a visual representation of the working half. Textures are indicated by the symbols shown in Figure 8. Two closely spaced horizontal lines in this column indicate the location of styrofoam spacers taped between basalt pieces inside the liner. Each piece is numbered sequentially from the top of each section, beginning with the number 1. Pieces are labeled on the rounded, not the sawed, surface. Pieces that could be fit together before splitting are given the same number, but are lettered consecutively (1A, 1B, 1C). Spacers are placed between pieces with different numbers but not between those with different letters and the same number. In general, the addition of spacers represents a drilling gap (no recovery). All pieces that are cylindrical and longer than the liner diameter have orientation arrows pointing up on both the archive and working halves. Special procedures ensure that orientation is preserved through every step

cm

0

50

100

150

Piece Number

Graphic Representation

Orientation

Shipboard Studies

Alteration

Piece Number

Graphic Representation

Orientation

Shipboard Studies

Alteration

1A

1B

2

T

DVP

M

CORE/SECTION

Site, core, sections, depth (m)  
Major rock type(s)  
Minor rock type(s)  
Macroscopic description(s)  
Thin section description(s)  
Shipboard studies

The code for these studies are:  
T = Thin section  
D = Density (g/cm<sup>3</sup>)  
V = Sonic velocity, either parallel (||) or perpendicular (⊥) to core axis  
P = Porosity (%)  
M = Magnetism  
NRM1 = Natural remanent magnetism (intensity × 10<sup>-4</sup>)  
NRM2 = Natural remanent magnetism (inclination in degrees)  
S.I. = Stable inclination (in degrees)

Figure 7. Form used to describe igneous rocks.

of the sawing and labeling process. All orientable pieces are indicated by upward-pointing arrows to the right of the graphic representation on the description forms. Because the pieces are rotated during drilling, it is not possible to sample for declination studies.

Samples are taken on board for various measurements. The types of measurements and approximate sample locations are indicated in the "Shipboard Studies" column by the following notation:

- M = magnetism measurement
- S = sonic-velocity measurement
- T = thin section
- D = density measurement
- P = porosity measurement

The state of alteration (see Fig. 8 for symbols) is shown in the "Alteration" column.

### Igneous and Metamorphic Rock Classification

Basalt was recovered on Leg 80. Classification is based mainly on mineralogy and texture. Basalts are termed aphyric, sparsely phyrlic, moderately phyrlic, or phyrlic, depending on the proportion of phenocrysts visible with the binocular microscope (about ×12). Basalts are called aphyric if phenocrysts are absent. For practical purposes, this means that if one piece of basalt was found with a phenocryst or two in a section where all other pieces lack phenocrysts, and no other criteria, such as grain size or texture, distinguish this basalt from the others, then it too is described as aphyric. The presence of rare phenocrysts is noted in the general description, however. This approach enables us to restrict the number of lithologic units to those with clearly distinct and persistent visible differences.

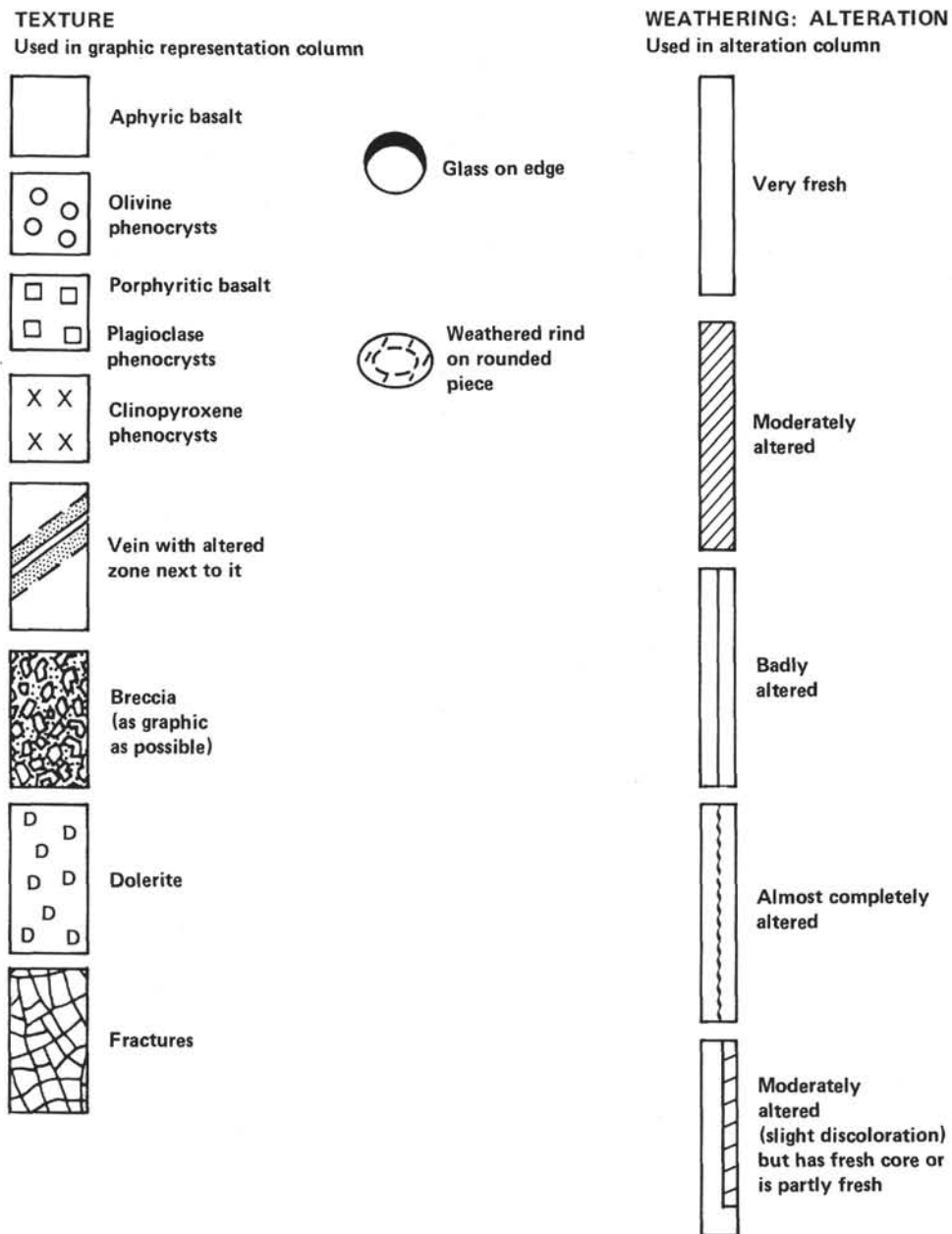


Figure 8. Symbols used to show the texture and alteration of igneous rocks.

Sparsely phyric basalts are those with 1 to 2% phenocrysts in almost every piece of a given core or section. Clearly contiguous pieces without phenocrysts are included in this category, and again the lack of phenocrysts is noted in the general description.

Moderately phyric basalts contain 2 to 10% phenocrysts. Aphyric basalts within a group of moderately phyric basalts are separately termed aphyric basalts.

Phyric basalts contain more than 10% phenocrysts. No separate designation is made for basalts with more than 20% phenocrysts; the proportion indicated in the core forms should be sufficient to guide the reader.

The basalts are further classified by phenocryst type, and a modifying term precedes such terms as phyric and sparsely phyric. A plagioclase-olivine, moderately phyr-

ic basalt contains 2 to 10% phenocrysts, most of them plagioclase but with some olivine.

### PHOTOGRAPHY

Both color and black and white photographs of whole cores are available for consultation. In addition, close-up black and white photographs of special structures are archived at DSDP.

### OBTAINING SAMPLES

Investigators who want to obtain core samples should refer to the DSDP-NSF Sample Distribution Policy at the front of this volume. Sample request forms may be obtained from the Curator, Deep Sea Drilling Project, A-031, University of California, San Diego, La Jolla,

Calif. 92093. Requests must be as specific as possible; include hole, core, section, interval within a section, and volume of sample required.

Requests for underway geophysical data should be sent to Manager, Data Group, Deep Sea Drilling Project, A-031, University of California, San Diego, La Jolla, Calif. 92093.

## REFERENCES

- Bartenstein, H., 1978. Paleontological zonation; parallelization of the lower Cretaceous stages in northwest Germany with index ammonites and index microfossils. *Erdoel Kohle*, 31(2):65-67.
- Bennett, R. H. and Keller, G. H., 1973. Physical properties evaluation. In van Andel, T. H., Heath, G. R., et al., *Init. Repts. DSDP*, 16: Washington (U.S. Govt. Printing Office), 521-528.
- Berggren, W. A., Kent, D. V., and Flynn, J. J., in press. Paleogene geochronology and chronostratigraphy. In Snelling, N. J. (Ed.), *Geochronology and the Geological Record*. Spec. Pap. Geol. Soc. London.
- Berggren, W. A., and Van Couvering, J. A., 1974. The late Neogene—biostratigraphy, geochronology and paleoclimatology of the last 15 million years in marine and continental sequences. *Palaeogeogr. Palaeoclimatol. Palaeoecol.*, 16:1-216.
- Bettenstaedt, F., 1952. Stratigraphisch wichtige Foraminiferen—Arten aus dem Barrême vorwiegend Nordwest-Deutschlands. *Senckenbergiana*, 33(4/6):263-295.
- Blow, W. H., 1969. Late middle Eocene to Recent planktonic foraminiferal biostratigraphy. In Brönnimann, P., Renz, H. H. (Eds.), *Proc. First Internat. Conf. Planktonic Microfossils*: Leiden (Brill), pp. 199-422.
- Boyce, R. E., 1976. Definitions and laboratory techniques of compressional sound velocity parameters and wet-water content, wet-bulk density, and porosity parameters by gravimetric and gamma ray attenuation techniques. In Schlanger, S. O., Jackson, E. D., et al., *Init. Repts. DSDP*, 33: Washington (U.S. Govt. Printing Office), 931-958.
- Bukry, D., and Bramlette, M. N., 1970. Coccolith age determinations, Leg 3, Deep Sea Drilling Project. In Maxwell, A. E., Von Herzen, R., et al., *Init. Repts. DSDP*, 3: Washington (U.S. Govt. Printing Office), 589-611.
- Čeppek, P., and Hay, W. W., 1969. Calcareous nannoplankton and biostratigraphic subdivision of the Upper Cretaceous. *Trans. Gulf Coast Assoc. Geol. Soc.*, 19:323-336.
- Clementz, D. M., Demaison, G. J., and Daly, A. R., 1979. Well site geochemistry by programmed pyrolysis. *Proc. 11th Annu. Off-shore Technol. Conf.* (Houston), pp. 465-470.
- Espitalié, J., Laporte, J. L., Madec, M., Marquis, F., Leplat, P., Poulet, J., and Boutefeu, A., 1977. Rapid method for source rock characterization and for evaluating their petroleum potential and their degree of evolution. *Rev. Inst. Fr. Pet.*, 32:23-42. (In French)
- Gealy, E. L., Winterer, E. L., and Moberly, R. M., Jr., 1971. Methods, conventions, and general observations. In Winterer, E. L., Riedel, W. R., et al., *Init. Repts. DSDP*, 7, Pt. 1: Washington (U.S. Govt. Printing Office), 9-26.
- Gieskes, J. M., and Rogers, W. C., 1973. Alkalinity determination in interstitial waters of marine sediments. *J. Sediment. Petrol.*, 43: 272-277.
- Hailwood, E. A., Bock, W., Costa, L., Dupeuble, P. A., Müller, C., and Schnitker, D., 1979. Chronology and biostratigraphy of north-east Atlantic sediments, DSDP Leg 48. In Montadert, L., Roberts, D. G., et al., *Init. Repts. DSDP*, 48: Washington (U.S. Govt. Printing Office), 1119-1142.
- Lynch, E. J., 1962. *Formation Evaluation*: New York (Harper and Row).
- Martini, E., 1971. Standard Tertiary and Quaternary calcareous nanofossil zonation. In Farinacci, A. (Ed.), *Proc. II Planktonic Conf.* (Vol. 2): Rome (Edizione Tecnoscienza), pp. 739-785.
- , 1976. Cretaceous to Recent calcareous nannoplankton from the central Pacific Ocean (DSDP Leg 33). In Schlanger, S. O., Jackson, E. D., et al., *Init. Repts. DSDP*, 33: Washington (U.S. Govt. Printing Office), 383-423.
- Matthews, D. J., 1939. *Tables of the Velocity of Sound in Pore Water and in Seawater*: London (Admiralty, Hydrographic Department).
- Müller, G., and Gastner, M., 1971. The "Karbonate-Bombe," a simple device for determination of the carbonate content in sediments, soils and other materials. *Neues Jahrb. Mineral. Monatsh.*, 10:466-469.
- Munsell Soil Color Charts*, 1971. Baltimore, MD (Munsell Color Company, Inc.).
- Poore, R. Z., 1979. Oligocene through Quaternary planktonic foraminiferal biostratigraphy of the North Atlantic: DSDP Leg 49. In Luyendyk, B., Cann, J. R., et al., *Init. Repts. DSDP*, 49: Washington (U.S. Govt. Printing Office), 447-517.
- Prell, W. L., Gardner, J. V., and Shipboard Scientific Party, 1982. Leg 68: introduction and explanatory notes, and conventions. In Prell, W. L., Gardner, J. V., et al., *Init. Repts. DSDP*, 68: Washington (U.S. Govt. Printing Office), 5-13.
- Schlumberger, 1969. *Log Interpretation Charts*: Houston (Schlumberger Ltd.).
- , 1972. *Log Interpretation* (Vols. I and II): Houston (Schlumberger Ltd.).
- Sigal, J., 1977. Essai de zonation du Crétacé méditerranéen à l'aide des foraminifères planctoniques. *Geol. Mediterr.*, 4(2):99-108.
- Stainforth, R. M., Lamb, J. L., Luterbacher, H., Beard, J. H., and Jeffords, R. M., 1975. Cenozoic planktonic foraminiferal zonation and characteristics of index forms. *Univ. Kans. Paleontol. Contrib. Pap.*, 62:1-425.
- Terzaghi, K., and Peck, R. B., 1967. *Soil Mechanics in Engineering Practice* (2nd ed.): New York (John Wiley and Sons, Inc.).
- Thierstein, H. R., 1973. Lower Cretaceous calcareous nannoplankton biostratigraphy. *Abh. Geol. Bundesanst.*, 29:1-52.
- , 1976. Mesozoic calcareous nannoplankton biostratigraphy of marine sediments. *Mar. Micropaleontol.*, 1:325-362.
- Wentworth, C. K. 1922. A scale of grade and class terms of clastic sediments. *J. Geol.*, 30:377-390.
- Wentworth, C. K., and Williams, H., 1932. The classification and terminology of the pyroclastic rocks: report of the Committee on Sedimentation. *Bull. Nat. Res. Council. U.S.*, 80:10-53.

Date of Initial Receipt: January 27, 1984

Date of Acceptance: February 27, 1984